Dijlah Journal of Engineering Science (DJES) Vol. 3, No. 2, June, 2026, pp. 1-8
ISSN: Printed: **3078-9656, Online: 3078-9664**, paper ID: 142

Convection heat losses in a parabolic trough solar collector's absorber tube as a function of wind speed: a CFD analysis

Khaleel Saleem Jebur Al-Ogaili
Department of mechanical engineering, Wasit University, Wasit, Iraq.

Article Info

Article history:

Received Oct., 20, 2025
Revised Jan.,7, 2026
Accepted Feb.,5, 2026

Keywords:

Parabolic trough solar collector, Receiver convection heat losses, Wind influence.

ABSTRACT

The receiver tube is an important part of the technology used in parabolic trough solar collectors (PTSCs). By changing the wind speed, this research develops a computational fluid dynamics (CFD) model of a PTSC receiver tube.The outside of the absorber tube should be 500k. This study aims to evaluate the influence of wind speed on convection heat losses in receiver tubes. The wind speed changed from 0 to 12 m/s. It has been shown that wind speeds below 6 m/s have a big effect on how much heat is lost by convection in receivers. However, the speed effect reduces at ranges greater than 6 m/s. The results of this investigation demonstrate the impact of wind speed ranges on convection heat losses in the PTSC receiver tube.

Corresponding Author:

Khaleel Saleem Jebur Al-Ogaili
Department of Mechanical Engineering, Wasit University,
Wasit, Iraq.
Email: Khaleel_msc@yahoo.com

1. INTRODUCTION

The receiver is one of the most important and expensive components in a Parabolic Trough Solar Collector (PTSC) power system [1]. Therefore, to improve PTSC power plants' performance and decrease heat loss from the absorber, many studies have mostly focused on investigating the influences of several factors on receiver operation. One of the ways to enhance PTSC performance is by using an absorber's selective coating to increase sunray absorption and decrease radiation power loss. Also, in order to reduce the heat losses, the annulus space between the absorber tube and the glass cover of the receiver is evacuated. Experimental, analytical, and numerical studies have been used to study the PTSC receiver's performance in a range of operating conditions [2-8]. Burkholder and Kutscher [2] investigated the heat loss of a PTSC model receiver as the temperature ranged from 100 to 500 °C. Khanna et al. employed an analytical method to show how the temperature changes along a PTSC absorber tube inside a PTSC system [3]. Cheng et al. utilized computer models to look at how heat moves through the PTSC receiver tube and how the solar flux is distributed unevenly out on the surface of the absorber tube [4]. Fluent and the MCRT method were used by Wu et al. [5]. Researchers looked into how the receiver surfaces' optical characteristics changed with wavelength and how much solar light they absorbed. Sahoo et al. [6] did a parametric numerical analysis of PTSC absorber tubes. They also modified the material of the absorber tube to see if the temperature around the tube was the same all the way around. Hachicha et al. [7] created an optical model to assist explain why energy moves weirdly around the receiver. The optical model's output was then used to set the boundary conditions for more heat transfer simulations using the Finite Volume Method (FVM). Odeh and Morrison created a simulation model to improve the PTSC system by adding a storage tank for use with industrial process heat (IPH) [8]. A transient analysis was employed to consider the variability of solar radiation. The researchers also used a collector that wasn't evacuated in their investigation to keep the cost of the receiver low. However, the influence of wind on the PTSC receiver tube convection heat losses was not addressed in the earlier research. Therefore, the primary focus of this study will be on the effects of wind on the PTSC receiving tube.

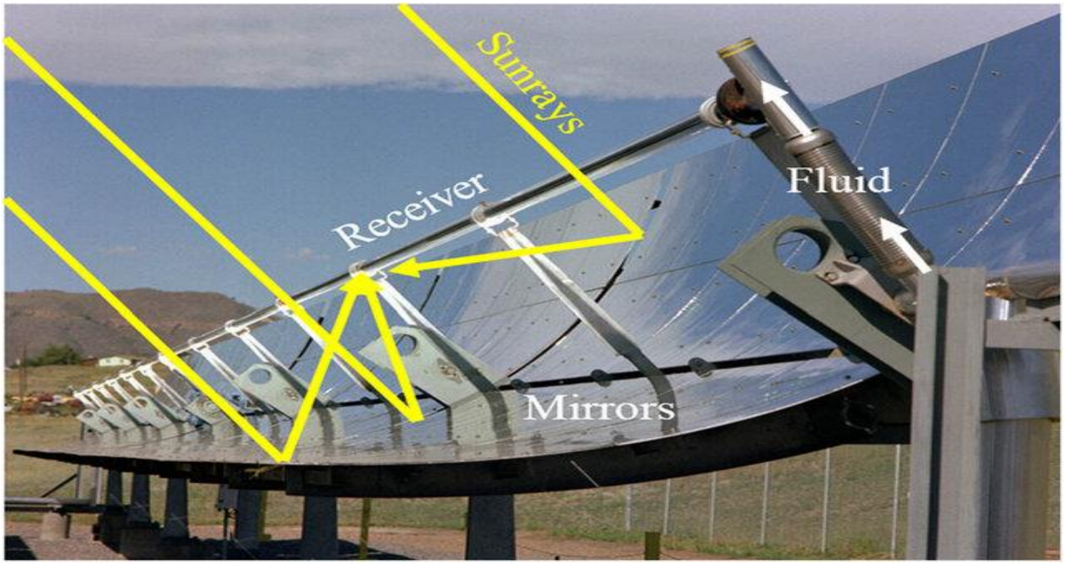

Figure 1. PTSC's Components [15]

2. Physical setup

Explaining In this work, the PTSC receiver's dimensions are maintained at a level comparable to the Sandia National Laboratory's LS-2 collector test [9]. Both the outer and inner diameters of the receiver's glass cover measure 0.115 and 0.109 meters, respectively. The absorber tube's diameters are 0.070 m on the outside and 0.066 m on the inside. The receiver is assumed to be 7.8 meters long. The outer diameter of the absorber tube is immediately exposed to temperature. The LS-2 module's design details are listed in Table [1].

Table 1: Information on the LS-2 collector that Sandia National Laboratory tested [2].

Character	PTSC's Parameter	Value	Unit
F	Focal length	1.84	M
W	Aperture width	5	M
L	Aperture length	7.8	M
D_{os}	Outer diameter of Receiver	0.070	M
D_{is}	Inner diameter of Receiver	0.066	M
D_{oc}	Diameter of outer glass Cover	0.0115	M
D_{ic}	diameter of inner glass Cover	0.109	M
E_c	Glass Cover thickness	0.006	M
K_s	thermal conductivity of the Absorber tube	54	W/m K
K_c	thermal conductivity of glass Cover	0.78	W/m K
A_{bs}	Absorber tube absorbance	0.96	-
E_c	Glass Cover emittance	0.86	-
C_{tr}	Glass Cover transmittance	0.95	-
C_{bs}	Glass Cover absorbance	0.02	-

3. Grid generation

The computational domain has been meshed using a hybrid meshing technique. The glass cover and absorber tube are examples of solid bodies that have been meshing automatically, while the HTF flow domain and annulus area are examples of fluid domains that have been meshing using tetrahedral elements. On the surfaces of the fluid domain that encounter solid surfaces, an inflating layer of hexahedral elements has been added in order to capture the surface heat transfer processes. Figure 2 displays the mesh that was created. The grid is refined in both longitudinal and circumferential directions to verify grid independence and validate current methods. Both longitudinal and circumferential refinements are done until the increase in HTF outlet temperature does not change.

ISSN: Printed: **3078-9656, Online: 3078-9664**, paper ID: 142

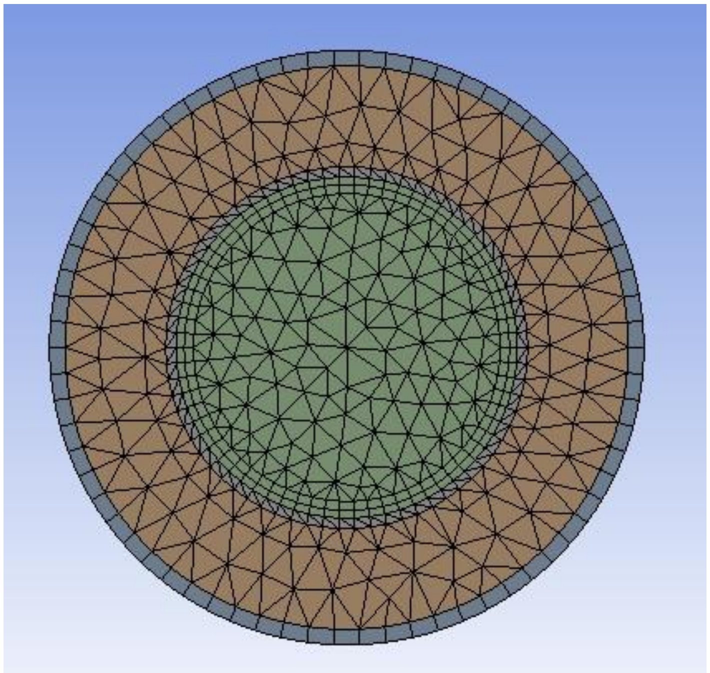

Figure 2. Diagram of The Created Mesh

4. Governing equations

The governing equations for steady flow, encompassing the conservation of mass, momentum, and energy, can be articulated as [11] for the HTF flow, characterized by a mass flow rate of 1 kg/s.

Continuity Equation:

$$\frac{\partial}{\partial x_i}(\rho \bar{u}_i) = 0 \quad \#(1)$$

Momentum Equation:

$$\frac{\partial}{\partial x_j}(\rho \bar{u}_i \bar{u}_j) = -\frac{\partial \bar{p}}{\partial x_i} + \frac{\partial}{\partial x_j}\left[\mu \left(\frac{\partial \bar{u}_i}{\partial x_j} + \frac{\partial \bar{u}_j}{\partial x_i} - \delta_{ij}\frac{\partial \bar{u}_l}{\partial x_l}\right) - \rho \bar{u}_i \bar{u}_j\right] \#(2)$$

Energy Equation:

$$\frac{\partial}{\partial x_j}(\rho \bar{u}_i C_p \bar{T}) = \frac{\partial}{\partial x_j}\left[\frac{\partial \lambda \bar{T}}{\partial x_j} + \frac{\mu_t}{pr_t}\frac{\partial C_p \bar{T}}{\partial x_j} + u_i\left(\mu\left(\frac{\partial \bar{u}_i}{\partial x_j} + \frac{\partial \bar{u}_j}{\partial x_i} - \frac{2}{3}\delta_{ij}\frac{\partial \bar{u}_l}{\partial x_l} - \rho \bar{u}_i \bar{u}_j\right)\right)\right] \#(3)$$

The heat transfer coefficient was calculated using Eq. 4.

$h = 4u_w^{0.58}\, D_{oc}^{-0.42}$ [12] (4)

Convection heat losses in the receiver tube are computed using Eq. 5

$Q_{conv} = hA_s(T_s - T_\infty)$ *[13]*

5. Boundary conditions and assumptions

After applying the right boundary conditions, the governing equations are solved. There was no sliding condition on the walls of the absorber tube. There is a boundary condition for the HTF that goes through the absorber tube at the mass flow inlet. The intake determined the characteristics of Syltherm 800 (HTF) [14]. The absorber tube exit has been set to zero-gauge pressure. The glass cover, annular zone, and sides of the absorber tube are all adiabatic, which means they don't emit or absorb radiation. The absorber tube and glass cover's characteristics, as listed in Table 2, are thought to be constant and unaffected by temperature. As an absorber surface boundary condition, the outside surface of the absorber tube is maintained at a constant temperature of 500°C. It is assumed that the absorber's end surfaces are adiabatic, and radiation losses through the absorber tube's input and outflow have been disregarded. Mixed boundary conditions are used to simulate convection and radiation from the glass cover into the surrounding air. It used equation (4) to figure out the effective heat transfer coefficient (h) for different wind speeds and then used that to calculate the glass surface's heat transfer coefficient. The air temperature is 300 K, while some people think the sky temperature is 295 K.A pressure-based steady-state solver was used to execute the simulations. The k-ε model and conventional wall functions are used to model turbulence. The SIMPLEC method was utilized to produce pressure-velocity coupling. A body force weighted technique was used to break up pressure into smaller parts, while a second-order upwind method was used to break up momentum, turbulent kinetic energy, turbulent dissipation rate, energy, and discrete ordinates. The equations for the continuity residuals, x, y, z velocity, k, ε, and DO intensity all need to come together at 10^{-4}. The energy equation needs to come together at 10^{-6}.

Table 2. The Glass Cover and Absorber Tube's Characteristics

Character	PTSC's Parameter	Value	Unit
Absorber tube	Density	8944	(kg/m3)
Glass Cover	Density	2225	(kg/m3)
Absorber tube	Specific Heat Capacity	0.39	(KJ/kgK)
Glass Cover	Specific Heat Capacity	0.835	(KJ/kgK)

6. Grid independence test

A test for grid independence has been done to discover the mesh value at which the output doesn't depend on the grid anymore. From 603345 to 1615636 elements, the grid's element count has been gradually raised. For each grid size being examined, the temperature rise of the HTF from inlet to outlet has been calculated while keeping all other factors the same. As the grid size is raised from 1578275 to 41615636, the observed HTF output temperature remains constant. Figure 3 displays the grid independence test results.

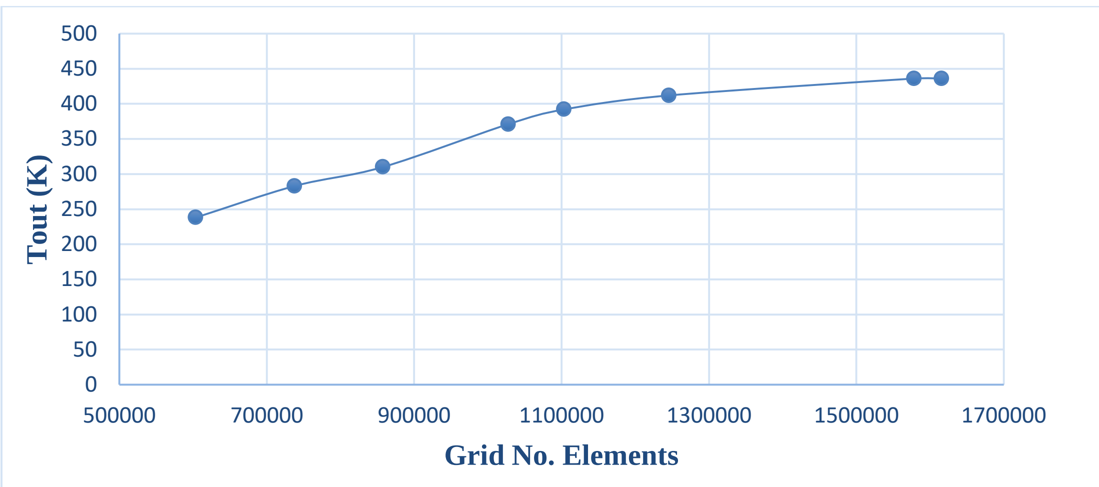

Figure 3. Grid Independence Test Results.

7. Results and discussions

This section of the study presents and describes numerical data in the form of graphs and figures to show how wind speed affects the temperature distribution of the receiver's glass cover and the convection heat losses of the receiving tube at different wind speeds. The cross-section of the glass-covered receiving tube's temperature contours under different wind speeds is shown in Table 4. The temperature contours for the glass cover were located near the centre of the tube's length. It is tested at u = 0, 2, 4, 6, 8, 10, and 12 m/s. It is clear that, especially at low wind speeds, the temperature of the glass cover decreased as wind speed increased. Wind speed more than 6 m/s has only a minor effect on the temperature of the glass cover. Additionally, Table 3 lists the temperature of the exterior glass as well as the variation in wind speed. The temperature of the receiving tube's glass cover reduced as expected as the wind speed increased from 0 to 12 m/s. It is evident from the figure that the glass cover dropped as the wind speed rose. This effect was most noticeable as the wind speed rose from zero to six meters per second. The effect of wind speed over 6 m/s on the temperature of the glass cover does, however, get weaker. It could be the temperature. Over time, the space between the glass cover and the air around it got narrower, so less heat was lost. The wind didn't influence the temperature of the glass cover as much.

ISSN: Printed: **3078-9656, Online: 3078-9664**, paper ID: 142

Table 3. At z = L/2, the temperature contours for the glass cover. For the values of u: 0, 2, 4, 6, 8, 10, 12, and 14 m/s.

Wind speed (m/s)	Glass cover temperature's contour
0m/s	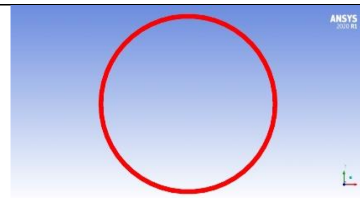
2 m/s	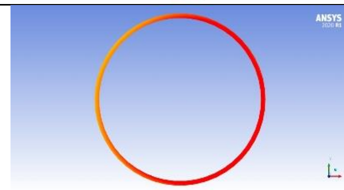
4 m/s	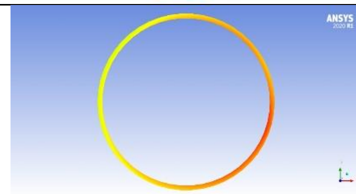
6 m/s	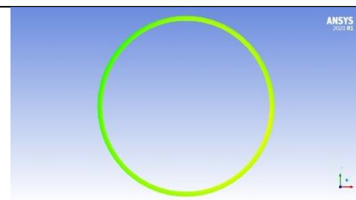
8 m/s	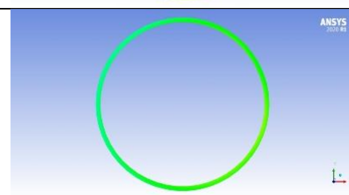
10 m/s	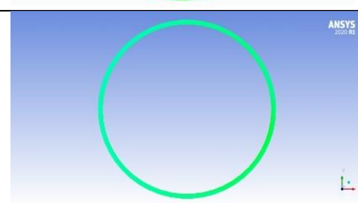
12 m/s	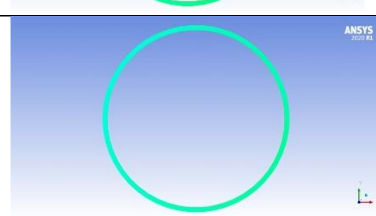

ISSN: Printed: **3078-9656, Online: 3078-9664**, paper ID: 142

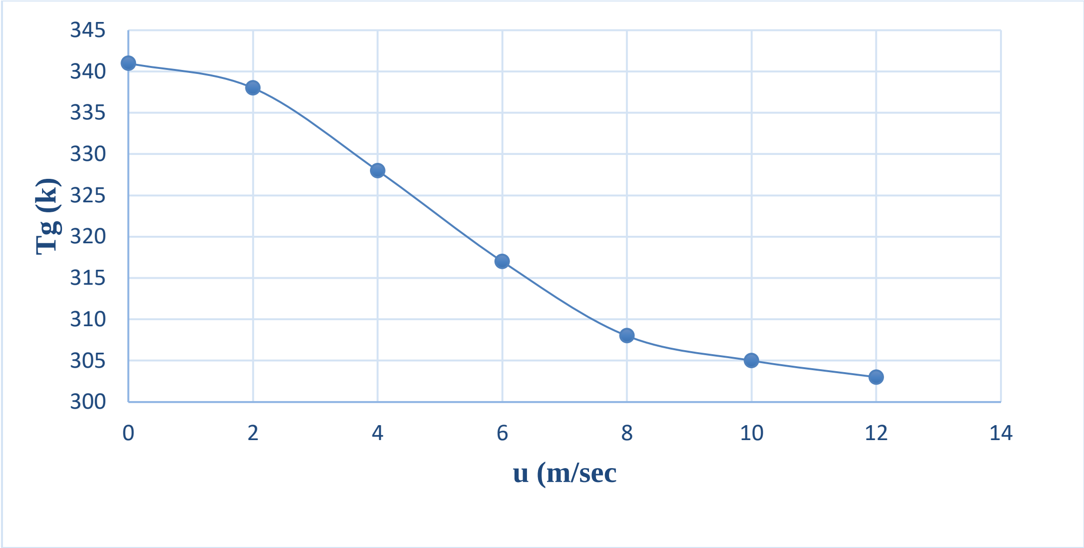

Figure 5. External Glass Temperature and Variation in Wind Speed

The influence of the receiving tube glass cover's convection heat transfer coefficient with wind speed fluctuation was demonstrated in Figure 6. As the wind speed varied from 0 m/s to up to 12 m/s, the figure makes it evident that the coefficient of convection heat losses grew significantly, leading to greater heat losses through the glass cover. Increased wind speed was the cause of this; in situations when the temperature differential between the wind and the cover glass stays relatively constant, the convection heat losses from the glass cover can be clearly increased.

Glass cover convection heat losses under a range of wind speeds, from 0 to 12 m/s, are shown in Figure 7. The increase in convection heat loss from zero to its maximum value at 2 m/s is obvious. The wind speed slowly dropped from 2 to 6 m/s. Heat losses from convection are roughly constant between 6 and 12 m/s. The coefficient of heat losses and the temperature difference between the glass and the wind are two of the factors that contribute to the volatility in convection heat losses from glass covers. The maximum value of 2 m/s is related to the greatest temperature difference between glass and wind. However, the remaining heat losses remain essentially constant, even as wind speed increases (from 6 m/s to 12 m/s) due to the small temperature differential between glass and wind.

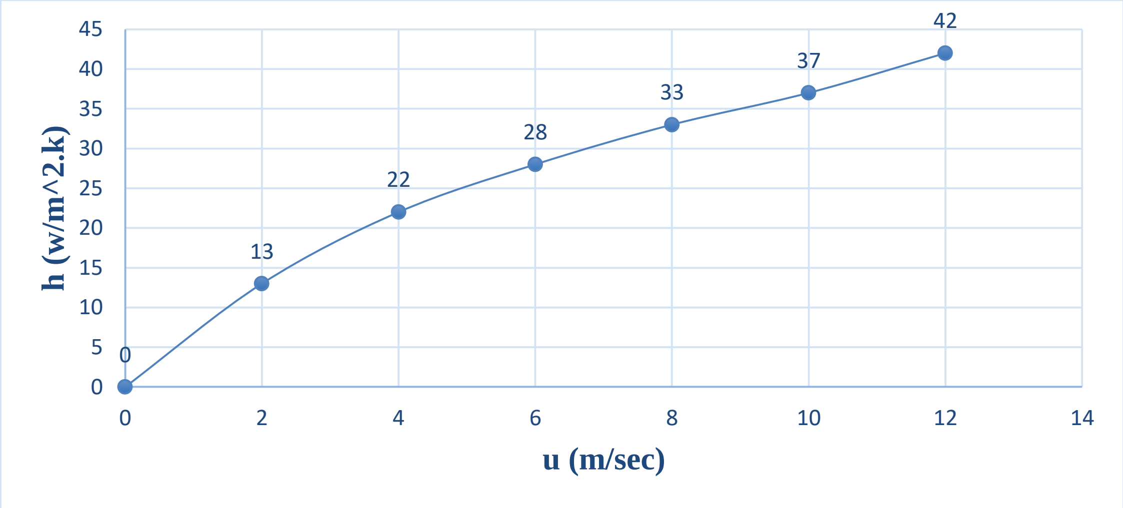

Figure 6. Convection Heat Transfer Coefficient and Varying Wind Speed

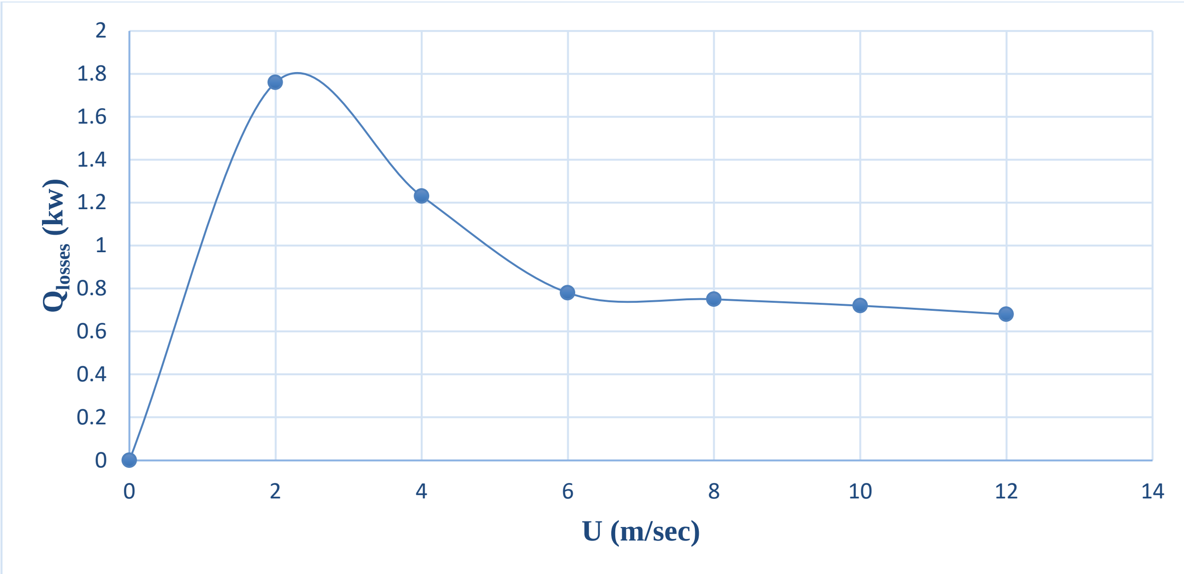

Fihure7. Convection Heat Transfer and Varying Wind Speed

8. Conclusion

A PTSC receiver tube's three-dimensional computational model was examined. Wind speed fluctuations across the glass cover were used in parametric simulations. Over the receiver glass cover, the wind speed ranged from 0 to 12 m/s. The HTF's entrance temperature was set at 300°K, while the collector absorber tube's outer surface temperature was set to 500°C. The findings of this study indicate that wind speed substantially influences PTSC performance by augmenting convection heat losses as wind speed rises. The coefficient of convection heat loss went up as the wind speed went up. This is why convection heat losses went up as the wind speed went up. However, for wind speeds more than 4 m/s, the wind's influence was found to decrease. At wind speeds above 6 m/s, the drop in convective loss value was generally consistent. This happened because the temperature differential between the glass and the wind got smaller and stayed almost the same, even though the glass reached a top speed of 2 m/s. The current study could be augmented for future research by integrating additional factors, including modifications in the absorber tube and glass cover thickness.

REFERENCES

[1] Byiringiro, J., Chaanaoui, M. and Hammouti, B., 2025. *Enhancement of thermal performance in parabolic trough solar Collectors: Investigation of three novel receiver configurations using advanced heat transfer fluids*. Solar Energy Materials and Solar Cells, 293, p.113833.

[2] Burkholder, F. and Kutscher, C., 2009. *Heat loss testing of Schott's 2008 PTR70 parabolic trough receiver* (No. NREL/TP-550-45633) . National Renewable Energy Lab.(NREL), Golden, CO (United States).

[3] Khanna, S., Singh, S. and Kedare, S.B., 2015. *Explicit expressions for temperature distribution and deflection in absorber tube of solar parabolic trough concentrator*. Solar Energy, 114, pp.289-302.

[4] Cheng, Z.D., He, Y.L., Xiao, J., Tao, Y.B. and Xu, R.J., 2010. Three-dimensional numerical study of heat transfer characteristics in the receiver tube of parabolic trough solar collector. International Communications in Heat and Mass Transfer, 37(7), pp.782-787.

[5] Wu, Z., Li, S., Yuan, G., Lei, D. and Wang, Z., 2014. *Three-dimensional numerical study of heat transfer characteristics of parabolic trough receiver.* Applied energy, 113, pp.902-911.

[6] Sahoo, S.S., Singh, S. and Banerjee, R., 2010. *Parametric studies on parabolic trough solar collector. Continuity*, 1(1), p.0.

[7] Hachicha, A.A., Rodríguez, I., Capdevila, R. and Oliva, A., 2013. *Heat transfer analysis and numerical simulation of a parabolic trough solar collector*. Applied energy, 111, pp.581-592.

[8] Odeh, S.D. and Morrison, G.L., 2006. *Optimization of parabolic trough solar collector system. International journal of energy research*, 30(4), pp.259-271.

[9] Behar, O., Khellaf, A. and Mohammedi, K., 2015. *A novel parabolic trough solar collector model–Validation with experimental data and comparison to Engineering Equation Solver (EES). Energy Conversion and Management,* 106, pp.268-281.

[10] Shajan, S. and Baiju, V., 2022. *Designing a novel small-scale parabolic trough solar thermal collector with secondary reflector for uniform heat flux distribution*. Applied Thermal Engineering, 213, p.118660.

[11] Cheng, Z.D., He, Y.L., Cui, F.Q., Xu, R.J. and Tao, Y.B., 2012. *Numerical simulation of a parabolic trough solar collector with nonuniform solar flux conditions by coupling FVM and MCRT method.* Solar Energy, 86(6), pp.1770-1784.

[12] Mullick, S.C. and Nanda, S.K., 1989. *An improved technique for computing the heat loss factor of a tubular absorber.* Solar Energy, 42(1), pp.1-7.

[13] Ratzel, A.C., Hickox, C.E. and Gartling, D.K., 1979. *Techniques for reducing thermal conduction and natural convection heat losses in annular receiver geometries.*

[14] Borzuei, D., Moosavian, S.F., Ahmadi, A., Ahmadi, R. and Bagherzadeh, K., 2021. *An experimental and analytical study of influential parameters of parabolic trough solar collector*. Journal of Renewable Energy and Environment, 8(4), pp.52-66.

[15] Tagle-Salazar, P.D., Nigam, K.D. and Rivera-Solorio, C.I., 2020. *Parabolic trough solar collectors: A general overview of technology, industrial applications, energy market, modeling, and standards. Green Processing and Synthesis*, 9(1), pp.595-649.

BIOGRAPHIES OF AUTHORS (10 PT)

The recommended number of authors is at least 2. One of them as a corresponding author.
Please attach clear photo (3x4 cm) and vita. Example of biographies of authors:

Dr. Khaleel Saleem Al-Ogaili, obtained a Ph.D. in Mechanical Engineering with a specialization in Solar Energy from the University of Southren quenslan / Australia (2019). He also holds a Master’s (2013)and a Bachelor’s (2004) degree in Mechanical Engineering from the University of Technology/ Iraq. He is currently a faculty member in the Department of Mechanical Engineering/ Wasit university.